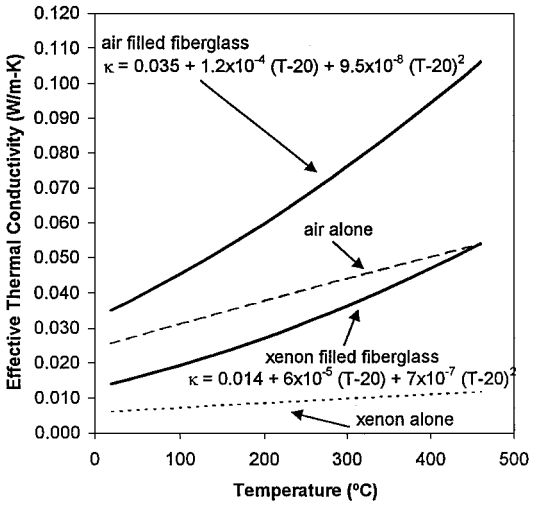

Fig. 3 Effective thermal conductivity vs temperature.

fiberglass insulation as a function of temperature. An equation of the form

$$k(T) = k_0 + a(T - T_0) + b(T - T_0)^2 \qquad (1)$$

was assumed for each gas, where T_0 was defined to be 20°C and the constants κ_0, a, and b determined by fitting the model output to the data of Fig. 2. As can be seen, reasonably good agreement was obtained by curve fitting the data in this fashion. The resultant $\kappa(T)$ functions are plotted and listed in Fig. 3. The xenon-filled fiberglass is seen to have roughly one-third the conductivity of air-filled fiberglass at room temperature and half the conductivity at 460°C. At 20°C both insulations are 0.008 W/m-K more conductive than their parent gases alone (Fig. 3), suggesting that the fiberglass itself contributes this amount to the overall conductivity. The fact that the gas-filled fiberglass conductivities increase with temperature more quickly than the parent gases alone is an indication of substantial radiative heat transfer at the higher temperatures. At 460°C the radiative component, as estimated by subtracting out the parent gas and fiberglass conductive components, is 0.034 W/m-K for xenon-filled fiberglass (63%) and 0.044 W/m-K (41%) for air-filled fiberglass. Note that both xenon heating curves in Fig. 3 have been fitted by the same $\kappa(T)$ function, demonstrating that the addition of aluminized Mylar did not reduce the radiative heat transfer.

Finally, the measured heat flux to the simulated payload was 84 W for the xenon-filled fiberglass and 189 W for the air-filled fiberglass at the simulated Venus surface temperature of 460°C. The xenon value therefore satisfies the original enclosure design target of being less than 100 W. A further 26 W for the xenon case and 46 W for the air case accumulate in the inner shell at this maximum 460°C external temperature to yield a total outside to inside heat flow of 110 and 226 W, respectively. Only 12 W of these totals is caused by conduction through the titanium struts.

Conclusions

Experimental data and analysis were presented for a prototype of a small, lightweight protective instrument enclosure for use near the surface of Venus. The novel features of the device included a concentric sphere geometry, xenon-gas-filled fiberglass insulation, and a low thermal conductance internal structure. Integrity of the overall structure under simulated Venus surface pressure and atmospheric entry deceleration loads was successfully demonstrated. Heating measurements yielded an effective thermal conductivity for the prototype for both xenon- and air-filled fiberglass insulation. For xenon this conductivity ranged from 0.014 W/m-K at 20°C to 0.054 W/m-K at 460°C. The net heat flow at 460°C to the simulated payload through xenon-filled insulation was 84 W, well within the required mission design goal of 100 W.

Acknowledgments

This research was carried out at the Jet Propulsion Laboratory, California Institute of Technology, under contract sponsored by NASA. Funding for this research was provided by the JPL Director's Research and Development Fund. The authors acknowledge and thank James Cutts of JPL's Special Project's Office for his guidance and Patrick O'Brien, Shannon Jackson, José Rivera, and Scott Leland, also of JPL, for their valuable technical assistance. National Technical Systems of Saugus, California, provided the high pressure and centrifuge test facilities for this project.

References

[1]Hughes Aircraft Company, *Pioneer Venus Case Study in Spacecraft Design*, AIAA, New York, 1979.

[2]Colin, L., and Hall, C. F., "The Pioneer Venus Program," *Space Science Reviews*, Vol. 20, D. Reidel, Dordrecht, The Netherlands, 1977, pp. 283–306.

[3]Jones, J. A., "Reversible Fluid Balloon Altitude Control Concepts," AIAA Paper 95-1621, May 1995.

[4]DiCicco, A. G., Nock, K. T., and Powell, G. E., "Balloon Experiment at Venus (BEV)," AIAA Paper 95-1633, May 1995.

[5]Lorenz, R. D., "Design Considerations for Venus Microprobes," *Journal of Spacecraft and Rockets*, Vol. 35, No. 2, 1998, pp. 228–230.

[6]Cutts, J. A., Kerzhanovich, V., Balaram, J., Campbell, B., Gershman, R., Greeley, R., Hall, J. L., Cameron, J., Klaasen, K., and Hansen, D. M., "Venus Aerobot Multisonde Mission," AIAA Paper 99-3857, June 1999.

[7]Heun, M. K., Jones, J. A., and Hall, J. L., "Gondola Design For Venus Deep Atmosphere Aerobot Operations," AIAA Paper 98-0897, Jan. 1998.

R. B. Malla
Associate Editor

Propulsive Efficiency of Hypersonic External Burning

G. E. Dorrington*
University of London,
London, England E1 4NS, United Kingdom

Introduction

THE idea of using external burning for propulsion in hypersonic flowfields has been proposed for various aerospace applications. Cuadra and Arthur,[1] for example, suggest external burning might be used for propulsive orbit plane change maneuvers. In the 1960s and 1970s, however, most interest in external burning appears to have been directed toward hypersonic cruise vehicles. In particular, Küchemann[2] discusses propulsive lifting bodies in support of his global transportation philosophy. Here Küchemann draws upon the theoretical studies of Oswatitsch[3] and Zierep[4,5] who derive linearized expressions for the propulsive efficiency of two-dimensional bodies with external burning in supersonic and hypersonic flows, respectively.

This Note briefly reintroduces the just-mentioned theoretical studies and sets out a simple isobaric slice analysis (ISA) method to obtain Oswatitsch's expression in a direct manner. The method is then extended to obtain an alternative approximation for propulsive efficiency in hypersonic flows, which sets a lower bound than indicated by Zierep. The approach used is believed to be original, although it bears some resemblance to an analysis by Gazley.[6]

Like the aforementioned works,[3–6] the ISA method assumes perfect gas relations. Real gas effects and viscous flow effects are ignored, and the simple analytical approximations developed here may

Received 2 December 1998; revision received 30 July 1999; accepted for publication 30 July 1999.

*Lecturer in Aerospace Design, Department of Engineering, Queen Mary and Westfield College.

only be used to indicate trends and to establish ideal performance limits.

Oswatitsch's Expression for Linearized Supersonic Flows

A flowfield with heat sources has a stream function, but no velocity potential in the accepted sense, because if heat is added, then the flow is no longer irrotational. Despite this obstacle, Oswatitsch[3] showed that a set of generalized flow equations can be obtained effectively by employing a generalized form of Crocco's theorem[7] linking vorticity with heat input and entropy gradient. After linearizing these generalized equations, Oswatitsch thereby deduced an expression for the propulsive efficiency η_p of a two-dimensional body with external heat addition in a supersonic flow with freestream velocity u_∞ and freestream Mach number $M_\infty = u_\infty / a_\infty$. The expression he obtained is

$$\eta_p = \frac{Fu_\infty}{\dot{m}q} = \frac{(\gamma - 1)\theta M_\infty^2}{\sqrt{\left(M_\infty^2 - 1\right)}} \tag{1}$$

where F is the thrust force produced on the body (which may be less than the overall drag on the body), $\dot{m}q$ is the total heat input rate, θ is the angle of the leading and trailing edges of the body (the flow deflection angle, assumed to be small), and γ is the ratio of specific heat capacities (of air).

Equation (1) clearly shows that within the range of applicability of the theory (i.e., within the supersonic range $\sqrt{2} > M_\infty < 5$) η_p increases with Mach number. However, even at the upper-supersonic limit, η_p is not large, e.g., $\eta_p \cong 0.1$ when $M_\infty = 5$, $\gamma = 1.4$, and $\theta = 0.05$.

Zierep–Küchemann Expression for Hypersonic Flows

Zierep extended Oswatitsch's analysis to heat addition in hypersonic flows[4,5] by assuming isochoric (constant volume) heat addition across fronts. In his analysis the increment in pressure across a front ΔP is proportional to the increment in heat added $\Delta P / P = \Delta q / (c_v T)$, where c_v is the specific heat capacity at constant volume and T is the temperature. The resulting expression[4,5] he obtained for η_p is

$$\eta_p = (\gamma - 1) M_1 \theta \tag{2}$$

where M_1 is the Mach number behind the shock attached to the leading edge of a two-dimensional body. Küchemann[2] plots this expression up to $M_\infty = 20$ and thereby indicates that high η_p is achievable. To do this, Küchemann employs approximate oblique shock relations[7] to define M_1 in terms of M_∞ and θ:

$$M_1 = M_\infty \Big/ \sqrt{\left[(3\gamma - 1)/(\gamma - 1) + \gamma(\gamma - 1) M_\infty^2 \theta^2 \right| \; 2\right]} \tag{3}$$

From this approximation Küchemann notes (as does Zierep) that when the hypersonic similarity parameter $M_\infty \theta$ is large (but θ remains small) the Mach number downstream of a hypersonic oblique shock tends to a limit:

$$M_1 \rightarrow (1/\theta)\sqrt{2/\gamma(\gamma - 1)} \tag{4}$$

i.e., Zierep's expression for η_p tends to a limit solely dependent on γ:

$$\eta_p \rightarrow \eta_{p\max} = \sqrt{2(\gamma - 1)/\gamma} \tag{5}$$

This result suggests promising values of η_p are feasible, e.g., when $\gamma = 1.4$ and $\eta_{p\max} \cong 0.76$.

Method for Supersonic Flows

Oswatitsch's expression for η_p can be more simply derived by assuming heat addition occurs at constant pressure.

In Fig. 1 a flat plate (viewed edgeways) is depicted. Isobaric heat addition is assumed to occur over some length l, near to the plate, in the region bounded by points 2-3-3′-2′. This heat release

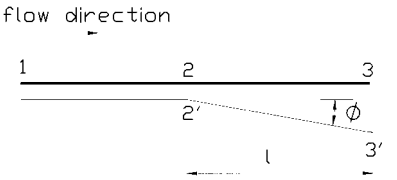

Fig. 1 Flat plate with isobaric heat addition.

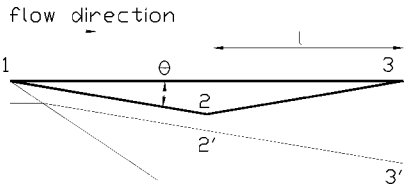

Fig. 2 Double wedge with isobaric heat addition.

causes an expansion of the flow such that the bounding streamline 2′-3′ is deflected by an angle ϕ, which is assumed to be small and constant. Because momentum is conserved in the isobaric region, the flow velocity between stations 2-2′ and 3-3′ is also constant. Hence, using the ideal gas equation

$$\rho_3 / \rho_2 = T_2 / T_3 = \delta / (\delta + l\phi) \tag{6}$$

where δ is the distance between the wall and the streamline defining the outer boundary of heat addition at point 2′ in Fig. 1. The required heat addition per unit mass flow (for a perfect gas with constant pressure specific heat capacity $c_p = \gamma c_v$) is therefore given by $q = c_p T_2 (T_3 / T_2 - 1) = c_p T_2 l\phi\delta$, and because the mass-flow rate being heated is $\dot{m} = \rho_2 u_2 \delta$, the heat input rate is

$$\dot{m}q = \rho_2 u_2 c_p T_2 l\phi \tag{7}$$

As Gazley suggests,[6] the (constant) pressure coefficient on the plate between stations 2-2′ and 3-3′ is the same as the pressure coefficient that would exist on a wedge of angle ϕ. For linearized supersonic flow (outside the heat addition zone) the standard Ackeret[8] expression can therefore be employed directly to obtain the pressure $P_{2\text{-}3}$ on the aft-body surface:

$$\frac{P_{2\text{-}3} - P_\infty}{\frac{1}{2}\rho_\infty u_\infty^2} = \frac{2\phi}{\sqrt{\left(M_\infty^2 - 1\right)}} \tag{8}$$

Eliminating ϕ from Eqs. (7) and (8), substituting $c_p T_2 = a_2^2 / (\gamma - 1)$, and ignoring the weak disturbance at station 2-2′ (such that $a_2 \cong a_\infty$, $u_{2\text{-}3} \cong u_\infty$), it follows that the normal lift force on the plate is given by

$$L_{2\text{-}3} = P_{2\text{-}3} l = \frac{(\gamma - 1) M_\infty^2}{\sqrt{\left(M_\infty^2 - 1\right)}} \dot{m}q / u_\infty \tag{9}$$

In Fig. 2 a two-dimensional double-wedge-shaped body (with the same geometry as that considered by Zierep[4,5]) is depicted with leading and trailing edges having the same small angle ϕ. Again, in the flow case depicted heat addition is assumed to be confined within an isobaric region defined by 2-3-3′-2′, but now the pressure on the aftbody face 2-3 is the same as on the forebody face 1-2 because in effect $\phi = 2\theta$. The normal lift force on the aft body is approximately the same as that given by Eq. (9) because θ is small, and the total lift force L will be double $L_{2\text{-}3}$ because the pressure rise on the forebody now has to be included. More pertinent, a thrust force is also exerted on the aft-body:

$$F \cong P_{2\text{-}3} l\theta \cong L_{2\text{-}3}\theta \tag{10}$$

which in this case balances the drag of the forebody. Hence, using the ISA method, η_p is found to be the same as Eq. (1) provided that the oblique shock emanating at angle β from the leading edge is

assumed to be weak, as will be the case for flows with low supersonic freestream Mach numbers.

Propulsive Efficiency at Higher Mach Numbers

At higher supersonic Mach numbers the Ackeret approximation just used becomes more inaccurate and must be replaced by oblique shock relations. In a hypersonic flow these relations remain valid (provided the leading edge is sharp), and they can be used to obtain the pressure $P_{1\text{-}3}$ on the underside of the double wedge depicted in Fig. 2. As the hypersonic similarity parameter $M_\infty\,\theta$ becomes large (but θ remains small), the relevant relations[7] are

$$\beta \to (\gamma + 1)\theta/2 \tag{11}$$

$$P_{1\text{-}3}/P_\infty \to 1 + \gamma\beta\theta M_\infty^2 \tag{12}$$

$$\frac{T_{1\text{-}2}}{T_\infty} \to \frac{2\gamma(\gamma-1)M_\infty^2\,\beta^2}{(\gamma+1)^2} \tag{13}$$

$$\rho_{1\text{-}2}/\rho_\infty \to (\gamma+1)/(\gamma-1) \tag{14}$$

For small θ the assumption can be made that $u_2 \cong u_\infty$; hence, combining Eqs. (11–14) with Eqs. (7) and (10), the η_p limit at very large freestream Mach numbers is

$$\eta_p \to (\gamma-1)/2\gamma \tag{15}$$

This asymptote is much less than the maximum limit deduced by Zierep, e.g., when $\gamma = 1.4$, Eq. (15) tends to about 0.14 rather than 0.76 as predicted by Eq. (5).

One reason for the difference between Eqs. (5) and (15) is that Zierep's analysis is restricted to small heat additions where the body still has net drag, whereas the scheme considered in Fig. 2 is effectively a cruise situation (ignoring skin friction) where thrust and forebody drag balance. When the hypersonic similarity parameter $M_\infty\,\theta$ is large, the drag on the forebody of the double wedge depicted in Fig. 2 is approximately $D = P_{1\text{-}2}\theta l$. The mass flow $\dot{m}$ being heated must lie within the leading-edge shock and so must be less than $\rho_{1\text{-}2}u_{1\text{-}2}l(\beta-\theta)$, i.e., using Eqs. (11) and (14), less than $(\gamma+1)\rho_\infty u_\infty l\theta/2$. Using Eq. (12), the net propulsive efficiency at this limiting mass-flow condition is therefore given by

$$\frac{(F-D)u_\infty}{\dot{m}q} \to \eta_{p\,\max} - \frac{\gamma M_\infty^2\,\theta^2 P_\infty}{\rho_\infty q} \tag{16}$$

Because Zierep[5] only strictly considers small additions across supersonic fronts such that $\Delta q \ll c_v T$, Eq. (16) must strictly be negative in the scheme he considers.

Another reason for the difference between Eqs. (5) and (15) is that the scheme considered above for the ISA method is not optimal. In Fig. 3 the dotted line represents the Mach line running from the trailing edge across the heated slice. The zone 3-3′-4 is not causally connected with the body, and so heat release in this zone is wasted. If heat release is restricted to the zone 2-3-4-2′, then the overall heat release might be reduced by some factor ε. To determine this factor, it is first necessary to consider the locus of the trailing-edge Mach line (Fig. 3).

Because $u_{2,3}$ is constant and T varies linearly with downstream distance in the isobaric slice, the Mach number M_r at radius r must

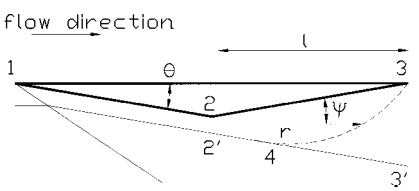

Fig. 3 Double wedge with truncated isobaric heat addition.

be $M_r \cong M_3\sqrt{(l/r)}$. And because at some angle ψ the local slope of the Mach line is $r\,\mathrm{d}\psi/\mathrm{d}r = -1/\sqrt{(M_r^2-1)}$, it follows that

$$\psi = \int_r^l \frac{\mathrm{d}r}{\sqrt{\left(M_3^2 lr - r^2\right)}} \tag{17}$$

The locus of the rear-connecting Mach line is therefore given by

$$r = \tfrac{1}{2}M_3^2 l[1-\cos(\psi_0-\psi)] \tag{18}$$

where $\psi_0 = \cos^{-1}(1-2/M_3^2)$.

The heat added can now be found by integrating across the truncated slice

$$\dot{m}q = \int_0^{2\theta} \rho_2 u_2 c_p T_2 r\,\mathrm{d}\psi$$

$$\cong \frac{1}{2}M_3^2\rho_2 u_2 c_p T_2 l[2\theta + \sin(\psi_0 - 2\theta) - \sin\psi_0] \tag{19}$$

Hence using Eq. (7), when $\phi = 2\theta$, the value of ε is given by

$$\varepsilon^{-1} \cong \tfrac{1}{2}M_3^2\{1 + [\sin(\psi_0-2\theta) - \sin\psi_0]/2\theta\} \tag{20}$$

Inspection of Eq. (18) shows that the maximum value for ψ that can be considered is $\psi_{\max} = \psi_0$, and hence $2\theta \le \psi_0$. Therefore the maximum feasible value of the ε factor is

$$\varepsilon_{\max}^{-1} \cong \tfrac{1}{2}M_2^3[1 - \sin\psi_0/\psi_0] \tag{21}$$

To first approximation, putting $\psi_0 \cong 2/M_3$, $\sin\psi_0 \cong 2/M_3 - (2/M_3)^3/6$, $\varepsilon_{\max} \cong 3$, and this maximum value occurs when $M_3\theta = 1$. Hence, even after the ε factor is taken into account, the extension of the ISA method to hypersonic flows still results in an upper limit on η_p that is significantly lower than Eq. (5), e.g., with $\gamma = 1.4$ the maximum η_p would be 0.42, still much less than Zierep's maximum value.

For hypersonic flows the ISA method yields a bound that is much closer to the numerical results of Broadbent.[5,9] Indeed, Broadbent[9] found it necessary to add a short cowl (near point 2′ in Fig. 3), effectively forming a scramjet, to achieve positive net propulsive efficiencies. Again this suggests the Zierep limit used by Küchemann is overoptimistic for (purely) external burning schemes intended to produce net thrust.

Conclusions

The ISA method presented herein may be used to obtain Oswatitsch's expression for the propulsive efficiency of external burning (propulsive lifting bodies) in a simple and direct manner. However, extension of the ISA method to hypersonic flows reveals a significant difference to Zierep's expression for propulsive efficiency, suggesting that Zierep's expression (as used by Küchemann) is overoptimistic for flight vehicles intended to produce net thrust.

References

[1] Cuadra, E., and Arthur, P. D., "Orbit Plane Change by External Burning Aerocruise," *Journal of Spacecraft*, Vol. 3, No. 3, 1966, pp. 347–352.

[2] Küchemann, D., *The Aerodynamic Design of Aircraft*, 2nd ed., Pergamon, Oxford, 1978, pp. 502–510.

[3] Oswatitsch, K., "Antriebe mit Heizung Bei Überschallgeshwindigkeit," DVL Bericht 90, Westdeutscher, Cologne, Germany, March 1959, pp. 1–29; also translation by K. E., Bücks, R.A.E. Library Translation, No. 811, March 1959, pp. 8–15.

[4] Zierep, J., "Über den Einfluss der Wärmerzufuhr bei Hyperschallströmungen," *Acta Mechanica*, Vol. 2, No. 2, 1966, pp. 217–230.

[5] Zierep, J., "Theory of Flows in Compressible Media with Heat Addition," Fluid Dynamics Panel of AGARD, AGARDograph 191, 1974.

[6] Gazley, C., "Linearized Solution for Heat Addition at the Surface of a Supersonic Airfoil," Rand Corp., Project Rand Research Memo. RM-1892, Santa Monica, CA, Nov. 1956.

[7] Cox, R. N., and Crabtree, L. F., *Elements of Hypersonic Aerodynamics*, 1st ed., English Universities Press, Ltd., London, 1965, pp. 17–35.

[8] Liepmann, H. W., and Roshko, A., *Elements of Gas Dynamics*, 1st ed., Wiley, New York, 1957, pp. 109–113.

[9]Broadbent, E. G., "Flows with Heat Addition," *Progress in Aerospace Sciences*, Vol. 17, No. 2, 1976, pp. 93–107.

J. A. Martin
Associate Editor

Closed-Form Equations to Evaluate Heat-Pipe-Cooled Leading-Edge Design Feasibility

David E. Glass*
AS&M, Hampton, Virginia 23666

Introduction

WHEN a thermal protection system designer is confronted with a leading-edge design for a hyersonic vehicle, the available options are either passively cooled, heat-pipe-cooled, or actively cooled systems. The upper use limit for passive leading edges may be determined by evaluating the material properties in light of the thermal and mechanical loads. If passive leading edges cannot survive the environmental conditions, heat-pipe-cooled or actively cooled leading edges may be required. Preliminary design studies at NASA Langley Research Center indicate that a refractory-composite/refractory-metal heat-pipe-cooled leading edge can reduce the leading-edge mass by over 50% compared to an actively cooled leading edge, can completely eliminate the need for active cooling, and has the potential to provide fail-safe and redundant features.[1] Though heat pipes are often a viable and lightweight option, the analysis required to determine the feasibility for a particular application can be extensive and can preclude their use. It is therefore beneficial to have a simple set of closed-form equations that can be used to determine if the heat-pipe option is feasible. Having a simple analysis technique available may prevent the unnecessary incorporation of active cooling systems when heat pipes may provide a cheaper and lightweight alternative and may also eliminate the need for a complex, three-dimensional finite element analysis (FEA) to answer the initial question of feasibility.

The purpose of this Note is to present a set of simple, closed-form design equations that can be used to determine a preliminary design of a heat-pipe-cooled leading edge. The design equations presented here are only for thermal design purposes and do not include any stress analysis. Temperatures obtained from the design equations are compared to three-dimensional for both a large and small leading-edge radius. Though some restrictions apply to the use of these equations, they appear to be a useful tool for the preliminary design of heat-pipe-cooled leading edges. Use of these equations will quickly answer questions such as, Is a heat-pipe-cooled leading edge even feasible? What is the heat pipe operating temperature? Are refractory metal or superalloy heat pipes required? Is a refractory-composite structure required? What is the required heat-pipe length? If the preliminary design equations indicate a feasible design, a more detailed analysis should follow.

Design Equations

The design of a heat-pipe-cooled leading edge is very complex because of the numerous variables involved. However, a simple set of closed-form equations is presented here that can be used to determine if a heat-pipe-cooled leading edge is feasible with various material combinations.[2] The equations presented here were developed to model the heat-pipe-cooled leading edge described in Ref. 3, but can be generalized for many other potential designs.

A schematic cross-section diagram of three heat pipes embedded in a structural material is shown in Fig. 1. The heat pipes shown in the figure have a rectangular cross section, but other cross sections could be considered. The leading edge is subjected to aerodynamic heating on the outer surface. At the stagnation line the location of maximum heating, the heating rate, is denoted by q''_{stag}. The thickness of the structure between the outer surface and the heat pipes is denoted by t_s, the outer coating thickness is t_c, and the heat-pipe container wall thickness is t_w. The distance between heat pipes is $2x$, and the width of the heat pipe is w. Contact resistance between the outer surface and the heat pipe is also noted in the figure. The contact resistance on the other surfaces of the heat pipe is of much less concern and is thus neglected. Two paths for the flow of heat from the region of maximum temperature T_{max} to the heat pipe are also shown in Fig. 1 using arrows.

Temperature Difference

The first step is to determine the temperature drop ΔT_{stag} through the structure and heat-pipe container at the stagnation line. This will help dertermine the maximum temperature of the leading edge (T_{max} in Fig. 1), which will occur on the outer surface at the stagnation line, midway between heat pipes. To determine the maximum temperature drop through the structure and heat-pipe container at the stagnation line, the following thermal resistances should be considered: through-the-thickness of the structure (from the outer surface to the heat pipe), in the plane of the structure (from midway between heat pipes to the heat pipe), and the contact resistance. If a coating is used on the outer surface, its thermal resistance (both in-plane and through-the-thickness) should be included. Two conduction paths are shown in Fig. 1 for the heat conducted from midway between heat pipes on the outer surface to the heat pipe. As shown, the heat must be conducted through the coating and structure in the through-the-thickness direction and through the coating and structure in the in-plane direction.

Figure 2 illustrates the approximation of the two-dimensional geometry of Fig. 1 with a thermal resistance network. The thermal resistance is for the heat conduction midway between heat pipes on the outer surface to the heat pipe. The through-the-thickness resistance in the structure is shown in Fig. 2 prior to the in-plane resistances but could be placed after the in-plane resistances with the same result. Other resistance networks could also be used, but care must be exercised because of inconsistent geometric areas. The thermal resistance through the heat-pipe container is neglected

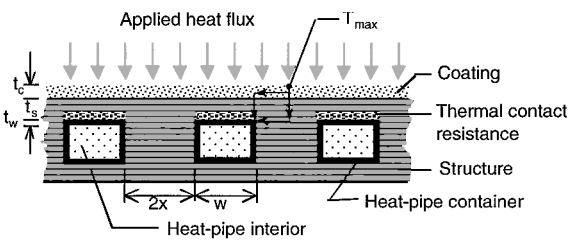

Fig. 1 Schematic of three heat pipes embedded in structure.

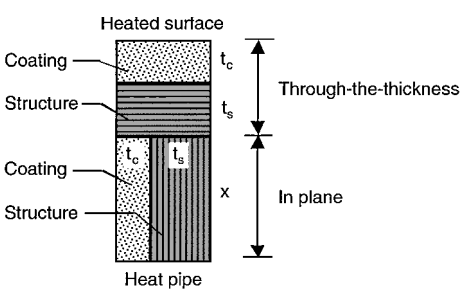

Fig. 2 Schematic drawing of the resistance network for heat to be conducted from midway between heat pipes on the outer surface to a heat pipe.

Received 3 June 1999; revision received 5 August 1999; accepted for publication 28 August 1999.

*Aerospace Engineer; currently TPS and Hot Structures Lead, Mail Stop 396, NASA Langley Research Center, Hampton, VA 23681. Associate Fellow AIAA.